HIGH-PRESSURE DROPLET COMBUSTION STUDIES

M. Mikami and M. Kono
Department of Aeronautics, University of Tokyo
Hongo, Bunkyo-ku, Tokyo 113, Japan

J. Sato
Research Institute
Ishikawajima-Harima Heavy Industries Co., Ltd.
Toyosu, Koto-ku, Tokyo 135 Japan

D.L. Dietrich
Sverdrup Technology, Inc.
NASA Lewis Research Center, Cleveland, Ohio 44135

and

F.A. Williams
Center for Energy and Combustion Research
Department of Applied Mechanics and Engineering Sciences 0310
University of California San Diego, La Jolla, California 92093

Introduction

This is a joint research program, pursued by investigators at the University of Tokyo, UCSD, and NASA Lewis Research Center. The focus is on high-pressure combustion of miscible binary fuel droplets. It involves construction of an experimental apparatus in Tokyo, mating of the apparatus to a NASA-Lewis 2.2-second drop-tower frame in San Diego, and performing experiments in the 2.2-second tower in Cleveland, with experimental results analyzed jointly by the Tokyo, UCSD, and NASA investigators. The project was initiated in December, 1990 and has now involved three periods of drop-tower testing by Mikami at Lewis.

The research accomplished thus far concerns the combustion of individual fiber-supported droplets of mixtures of n-heptane and n-hexadecane, initially about 1 mm in diameter, under free-fall microgravity conditions. Ambient pressures ranged up to 3.0 MPa, extending above the critical pressures of both pure fuels, in room-temperature nitrogen-oxygen atmospheres having oxygen mole fractions X of 0.12 and 0.13. The general objective is to study near-critical and super-critical combustion of these droplets and to see whether three-stage burning, observed at normal gravity, persists at high pressures in microgravity. Results of these investigations will be summarized here; a more complete account soon will be published (ref. 1).

Experimental Apparatus and Procedure

Figure 1 shows a schematic diagram of the experimental apparatus. The pressure chamber has four orthogonal windows that give two views of the combustion process, a backlit view from which the droplet size as a function of time is obtained and a second view which shows

the flame surrounding the droplet. During each test, both of these views were recorded by 16 mm cine cameras. Microgravity conditions were attained by dropping the pressure chamber and associated experimental equipment in a drop tower at NASA Lewis Research Center that provides 2.2 seconds of microgravity ($\sim 10^{-5}$ normal).

Before release of the experimental package, a fuel droplet was formed at the end of a 0.125 mm silica fiber from a high-pressure syringe driven by a stepping motor. Following release, immediately upon entry into microgravity the droplet was ignited. The ignition source was a hot wire (aluminum alloy, 0.2 mm diameter) formed into a 2 mm diameter loop that surrounds the droplet. The hot wire was rapidly removed after ignition, leaving approximately 2 sec of the 2.2 sec to observe combustion. All processes, including droplet dispensing and ignition, were controlled by a microcomputer.

The initial droplet size was approximately 1 mm in diameter.[1] This droplet diameter is nearly an order of magnitude larger than that of the suspending fiber, while also being small enough that complete burning could be observed in the available microgravity time. The ambient gas was a nitrogen-oxygen mixture with oxygen mole fractions, X, being 0.12, except for a small number of tests at X = 0.13. These reduced oxygen concentrations were employed to aid in visualizing the droplet from the backlit view at high pressure. All experiments were performed with the ambient gas and the droplet initially at room temperature.

The binary fuel droplet was composed of n-heptane and n-hexadecane with mass fractions of hexadecane, Y, ranging from 0 (pure heptane) to 1.0 (pure hexadecane). The subject fuels have critical temperatures and pressures of 540 K, 2.74 MPa and 722K, 1.53 MPa for heptane and hexadecane respectively. The pressure in the data reported here varied from 0.4 to 3.0 MPa.

General Combustion Behavior

Figure 2 shows variations of the square of the droplet diameter d with time t at different pressures, both normalized according to theory by dividing by the square of the initial droplet diameter d_o. For fuel mixtures, after the initial transition period and the first stage of linear behavior, another transition period exists (the second stage), after which the square of the droplet diameter again decreases with time almost linearly (the third stage), as seen in Figure 2. The cause of such three-stage burning is as follows: In the first straight segment, the high-volatility fuel, heptane, vaporizes preferentially from the droplet surface since the droplet temperature is relatively low. Since liquid-phase diffusion is slow relative to droplet surface regression, the hexadecane mass fraction gradually increases in the surface region. When the surface concentration of hexadecane reduces that of heptane sufficiently, the vaporization rate decreases and the flame approaches the droplet (the second transition period). After the droplet is heated by the flame enough to allow sufficient hexadecane to vaporize, hexadecane and heptane vaporize vigorously together, in the second straight segment. Figure 3, which shows both normalized droplet diameter and flame diameter as functions of time, illustrates how flame contraction follows the onset of the transition period; this delay is reduced at larger X.

[1] When the droplet is suspended from the fiber, it is not spherical in shape, but is elongated along the fiber due to surface tension. The equivalent spherical droplet diameter is computed as the cubic root of the product of the major diameter (along the fiber) with the square of the minor diameter (perpendicular to the fiber).

As seen in Figure 2, this staged type of burning still exists at the supercritical ambient pressure of 3 MPa. The concentration Y=0.11 in Fig. 2 lies outside the boundary of staged burning reported earlier by Niioka and Sato. The phenomenon may have been present but not observable in the normal-gravity experiments because the duration of the second stage is shortened by the increased rate of heat transfer produced by natural convection, or the gas-velocity and surface-tension variations under natural convection may have promoted internal liquid mixing and thereby narrowed the region of staged burning. Stage burning occurred for all mixtures tested other than pure fuels in the present study.

Homogeneous nucleation is not observed in this experiment. This result is expected because the ambient gas is diluted with nitrogen, reducing the droplet surface temperature, so that the local droplet temperature has less of a tendency to exceed the limit of superheat.

Droplet Lifetime

Figure 4 shows the dependence of the normalized droplet lifetime[2], t_l, at different ambient pressures on the initial hexadecane mass fraction.

This figure shows that the droplet lifetime reaches a maximum at an intermediate hexadecane mass fraction, at all but the highest pressure. For fixed initial hexadecane mass fraction, the droplet lifetime decreases with increasing ambient pressure, except for pure hexadecane. For hexadecane, the droplet lifetime exhibits a minimum value at 2.5 MPa rather than the critical pressure of 1.5 MPa, and the burning-rate constant exhibits a maximum at 2.5 MPa, as described later. Earlier results indicated that in air the burning-rate constant achieves its maximum at the critical pressure. Studies of fuel-droplet evaporation, however, have reported that the evaporation constant reaches its maximum at an ambient pressure above the critical pressure and at higher ambient pressures when the ambient temperatures are lower. Therefore, the occurrence of the minimum droplet lifetime and the maximum burning-rate constant above the critical pressure, rather than near the critical pressure, may be caused by delayed attainment of liquid criticality, associated with the lower temperatures produced by dilution of air in the present experiments. It is noteworthy that minima are not seen for heptane or any of the mixtures. Most of their histories seem dominated by heptane, whose critical pressure is significantly higher; the minima could develop at higher pressures for these droplets.

As shown by Figure 2, the square of the droplet diameter decreases almost linearly with time in the first and third stages. Figure 5 shows the burning-rate constant in the first stage, K_1, and in the third stage, K_3, both here defined from the maximum slope in each segment. While K_1 decreases sharply with increasing initial hexadecane mass fraction at fixed ambient pressure, K_3 increases somewhat. Both increase with increasing pressure, except for pure hexadecane, which exhibits a maximum value at 2.5 MPa, as described above.

Since the first straight segment occupies most of the droplet lifetime for small Y, K_1, which decreases with increasing Y, has a major influence under these conditions. On the other hand, for large Y, since the second straight segment occupies most of the droplet lifetime, K_3, which increases with increasing Y, is dominant.

The burning-rate constant K_1 may be approximated as

$$K_1 = [8\lambda/(\rho c_p)]ln(1+B) \tag{1}$$

[2]The droplet lifetime is defined as the time from the initial appearance of a luminous flame until the droplet disappears.

where the transfer number B is

$$B = [Y_{C7+} + Y_{O,\infty}\, \nu_{C7}\, W_{C7}/(\nu_O W_O)]/(1 - Y_{C7+}) \tag{2}$$

on the assumption that, in the first straight segment, the droplet surface temperature is nearly equal to the boiling point of heptane, and hexadecane vaporization is negligible for small hexadecane mass fraction. Here, Y_{C7+} is heptane mass fraction in the gas phase at the gas-liquid interface. The heptane mole fraction in the gas phase X_{C7+} is written as

$$X_{C7+} = \alpha X_{C7-} = \alpha(1 - X_{C16-}) \tag{3}$$

by Raoult's law and the Clausius-Clapeyron relation, where $\alpha < 1$, and X_{C7-} and X_{C16-} are heptane and hexadecane mole fractions in the liquid phase at the phase interface. Here Y_i are related to X_i as

$$Y_i = X_i W_i / \Sigma X_j W_j \qquad . \tag{4}$$

From these relations, $dK_1/dY_{C16-} < 0$ can be shown, which is consistent with the decrease in K_1 with increasing initial hexadecane mass fraction.

Similar reasoning could rationalize the K_3 dependence only if heptane vaporization were negligible in the third stage. It seems more likely that, with decreasing Y, the reduced duration of the third stage delays attainment of its maximum K_3.

Onset of the Second Transition Period

Figure 6 shows data for the ratio of the critical volume, V_c, defined as the volume of the droplet at the onset of the second transition period, to V_o, the initial droplet volume. These data also may be interpreted approximately as the volume at the onset of flame contraction, which follows the onset of the transition period as seen Figure 3. Results at an ambient oxygen mole fraction of 0.13 are also shown in Figure 6. The results indicate that the critical volume increases with the initial hexadecane mass fraction and is almost independent of ambient pressure and oxygen content.

Two types of curves are shown in Figure 6 for the critical volumes at 1 MPa generated with different assumptions. The dotted curve is

$$V_c/V_o = Y(\rho_o/\rho) \tag{5}$$

on the assumption that the liquid-phase diffusion is infinitely rapid and hexadecane does not vaporize until the droplet has exhausted all heptane. Here ρ_o is the density of the fuel mixture at room temperature, and ρ the density of hexadecane at the boiling point of heptane. The broken curves are

$$V_c/V_o = [Y/\{Y + 3\epsilon(1 - Y)\}](\rho_o/\rho), \tag{6}$$

which is an equation of Shaw based on the assumption that the liquid-phase diffusion coefficient D is sufficiently small relative to the burning-rate constant K such that $\epsilon = 8D/K << 1$ can be treated as a small parameter, and hexadecane vaporization is negligible. If ϵ is estimated with the assumption that D is the liquid-phase diffusion coefficient of heptane in hexadecane at the boiling point of heptane, and K is the burning-rate constant of heptane, then at 1 MPa, ϵ is about 0.05. The experimental results lie between this result and the infinite-diffusivity result but fall closer to this result at the larger values of Y and closer to the infinite-diffusivity curve at smaller Y. Reasons for this behavior are discussed fully in ref. 1.

Conclusions

The main conclusions can be listed: Staged burning still exists above the critical pressures of heptane and hexadecane. Heptane is dominant in gasification in the first stage and hexadecane in the third even at high pressure. Droplet lifetimes increase with the initial hexadecane mass fraction and reach a maximum value at a mass fraction of about 0.3 for pressures below 2.5 MPa in sufficiently diluted atmospheres. The maximum burning-rate constant in the first stage decreases with the initial hexadecane mass fraction but that in the third stage increases. The droplet volume at the onset of the second transition period is almost independent of the ambient pressure. Although it can be predicted qualitatively from liquid-phase diffusion-controlled theory, quantitative predictions are uncertain because of variations in burning-rate constants and in liquid-phase diffusion coefficients.

Future Plans

In view of the results described above, it would be of interest to test behaviors of these mixtures at higher pressures and at different oxygen-nitrogen ratios, particularly at higher oxygen content, such as in normal air. However, experimental difficulties in observing the droplets cause the success of such investigations to be uncertain. Other plans under consideration involve studying free droplets, testing binary alcohol mixtures at these elevated pressures (but probably not super-critical because of their higher critical pressures), and investigating droplet arrays to obtain information relevant to high-pressure spray combustion. In any event, this successful international cooperation appears to deserve to continue.

References

1. Mikami, M., Kono, M., Sato, J., Dietrich, D.L., and Williams, F.A., "Combustion of Miscible Binary-Fuel Droplets at High Pressure under Microgravity," Combustion Science and Technology, to appear, 1992.

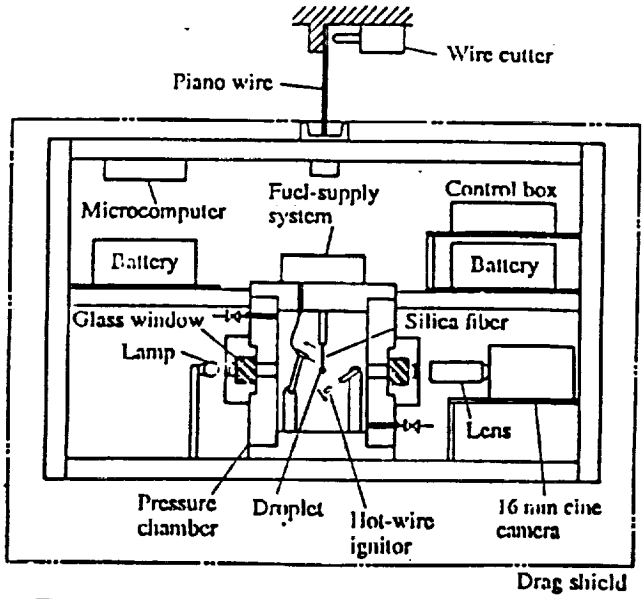

Figure 1. Schematic diagram of the experimental apparatus.

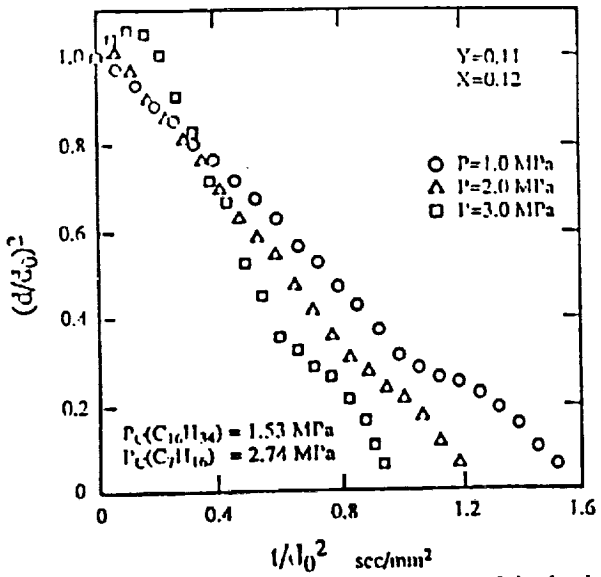

Figure 2. Temporal variation of the square of the droplet diameter, d, with time at different ambient pressures.

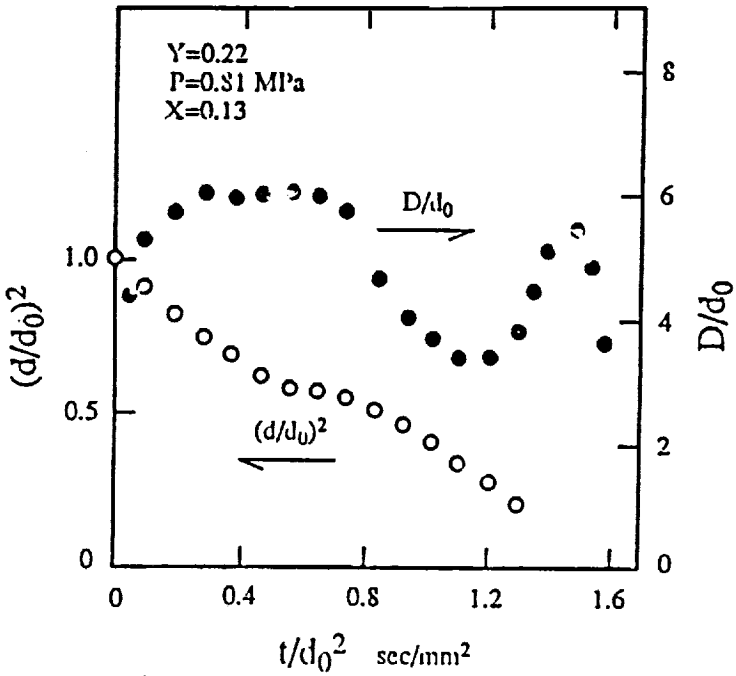

Figure 3. Temporal variations of the square of the droplet diameter, d, and flame diameter, D, with time.

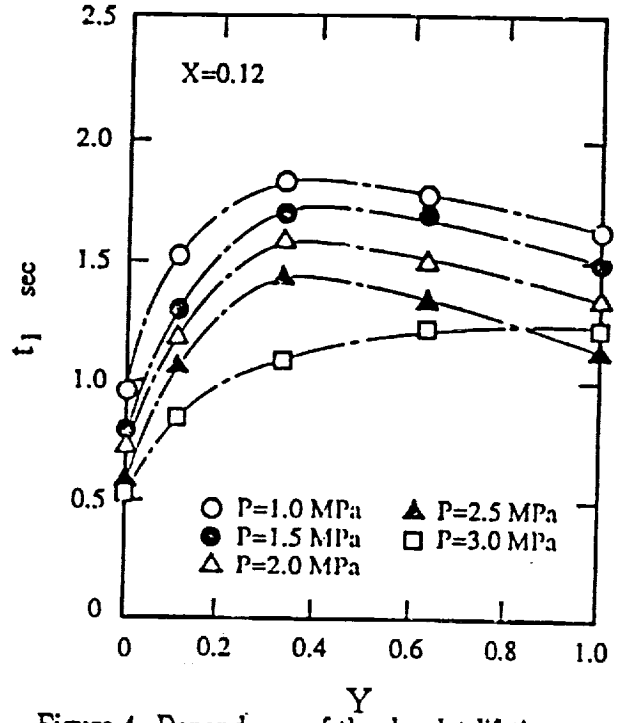

Figure 4. Dependence of the droplet lifetime, t_l, at different ambient pressures on the initial hexadecane mass fraction, Y.

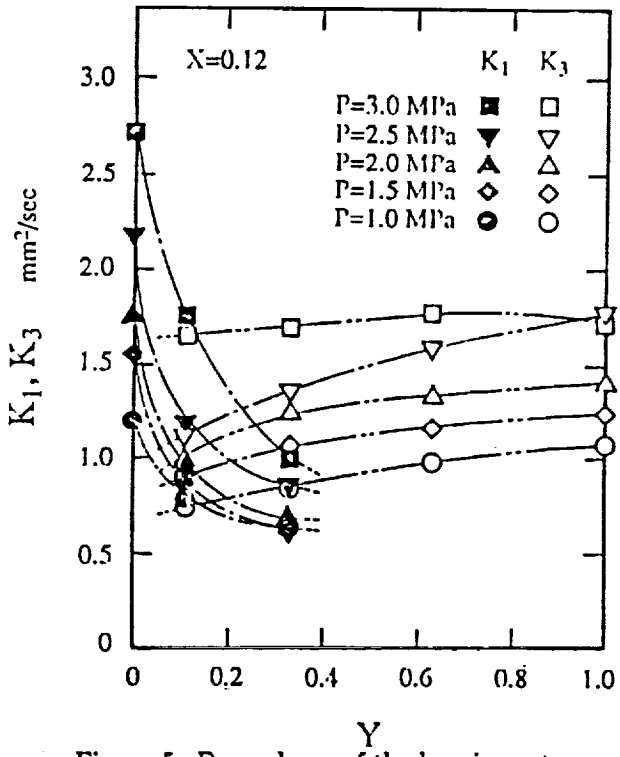

Figure 5. Dependence of the burning rate constant in the first stage, K_1, and in the third stage, K_3, at different ambient pressures on the initial hexadecane mass fraction, Y.

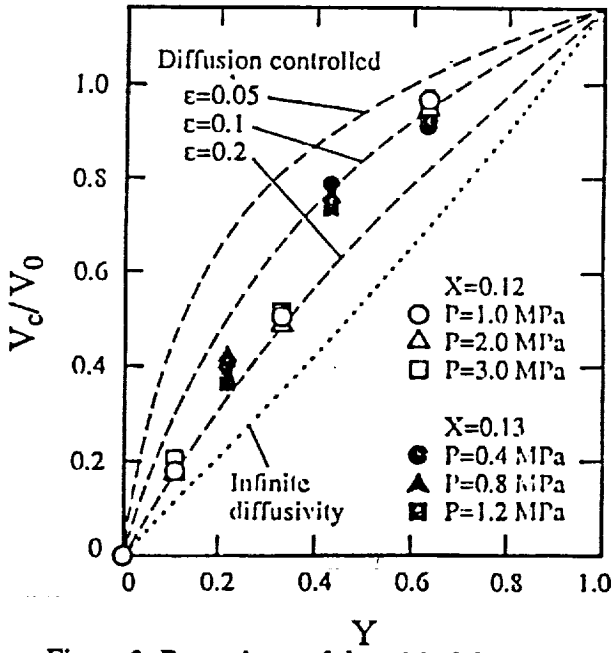

Figure 6. Dependence of the critical droplet volume, V_c, at different ambient pressures on the initial hexadecane mass fraction, Y.